Exchange flow of oil and sea-water in a ruptured submarine pipeline

C. Kranenburg

Report no. 1 - 83

Laboratory of Fluid Mechanics
Department of Civil Engineering
Delft University of Technology

EXCHANGE FLOW OF OIL AND SEA-WATER IN A RUPTURED SUBMARINE PIPELINE

C. Kranenburg

Report no. 1-83

Laboratory of Fluid Mechanics
Department of Civil Engineering
Delft University of Technology
Delft, The Netherlands

1983

Abstract

The rupture of a submarine oil pipeline starts various mechanisms leading to an oil spill. Among these mechanisms the leakage of oil driven by the difference in specific gravities of oil and sea-water is difficult to quantify. A simple mathematical model has been developed and laboratory experiments have been carried out to obtain an insight into the density-driven exchange flow in a pipeline initially completely filled with oil, and to determine the leak rate. The mathematical model is predictive and takes account of various relevant effects, such as those of friction and inclination of the pipeline. The experiments were done in a horizontal model pipeline. Theoretical and experimental results are in satisfactory agreement.

Contents

1. Introduction

One of the hazards concerning the exploitation of a submarine oil pipeline is formed by the possibility of rupture of the pipeline, as a consequence of an anchor being dragged by a ship, for example. The resulting oil spill is a potential source of damage to the environment. It is convenient to divide the origins of oil loss from a ruptured pipeline into two categories. The first category is characterized by a relatively short duration (e.g., up to fifteen minutes) and high leak rates. This category includes loss caused by the finite response time of the automatic shut-down system, compressibility loss and loss owing to initial momentum of the oil. The losses of this category can be estimated reasonably well (2). The second category comprises loss of oil as a result of an exchange flow of oil and sea-water, and is characterized by a long duration and relatively low leak rates. The loss of the second category can form a substantial part of the total loss, but cannot be estimated in a comperably simple way as the losses of the first category. A theoretical and experimental analysis of the exchange flow and related leak rate is presented in this report.

The exchange flow comes into existence when the pressures in the pipe and the sea-water have become approximately equal, and is driven by the difference in specific gravities of oil and sea-water. The heavier sea-water intrudes in the lower part of the pipeline, and the oil flows out at the top (figure 1.1). The leak rate can be influenced by:

- inner diameter, inclination and length of the pipeline,
- geometry of the rupture,
- specific gravities of oil and sea-water,
- viscosities of oil and sea-water, and, on small scales,
- interfacial tension.*

The inclination of the pipeline to the horizontal can act as a trap to the intrusion process: the intruding sea-water will be blocked in an upward sloping pipeline, if the pipeline rises by more than one diameter. On the other hand, a downward slope increases the flow rates. In general, oil will leak from both sides of the rupture. The size and shape of the

---

*Interfacial tension is the equivalent of surface tension at a free surface.

rupture, and possible entrance losses set an upper bound to the leak rate. It is assumed throughout this study that the ruptured pipe is cleanly cut through (figure 1.1), and that both sides of the rupture do not influence each other.

Initially the exchange flow is controlled by the inertia of the fluid. In later stages of the exchange process viscous or turbulent friction can gradually decrease the leak rate. Interfacial tension is of minor importance for prototype pipelines, but can substantially reduce the leak rate in small-scale models.

This report presents a simple mathematical model of the exchange process in a pipeline initially completely filled with oil that takes account of the effects mentioned (section 2), and describes experiments using a large, horizontal model pipeline (section 3). The results of theory and experiment are compared in section 4. The influence of interfacial tension in a small-scale model described in (3) is also shown. In section 5 some theoretical results are given for the prototype pipeline from the Q-1 block in the Dutch sector of the North Sea to IJmuiden. The study ends with a set of conclusions (section 6).

2. Simple mathematical model

The mathematical model presented below is based on the integral conservation laws of mass and momentum in the two-layered flow of oil and sea-water. Various assumptions to simplify the model are made, the more important ones being:

- the Boussinesq approximation for small density-differences may be applied,
- the circular cross-section of the pipeline may be approximated by a square,
- the oil is a newtonian fluid with constant viscosity and constant density; the flow in the oil layer remains laminar,
- the friction in the water layer, when turbulent, is given by the Blasius law for a smooth wall (section 2.5),
- the mean level of the interface with respect to the pipe wall is constant and may be determined so that the friction effect is minimal (section 2.2),
- the front or head (figure 1.1) of the intruding water layer may be modelled as is usual in the case of saline and fresh water (section 2.3), and

- the pipeline is infinitely long and has a constant (small) inclination, or is horizontal.

Interfacial tension is included in the model to demonstrate its effect in small-scale models. The system of equations derived is closed in that no use is made of adjustable parameters. The equations were solved numerically.

2.1. Equations of continuity and motion

The local equations of continuity are (figure 2.1)

$$\frac{\partial a_2}{\partial t} + \frac{\partial}{\partial x} a_2 u_2 = 0 \qquad (2.1.1)$$

and

$$a_1 u_1 + a_2 u_2 = 0 \qquad (2.1.2)$$

where t is time, x the coordinate along the pipeline, a_1 (a_2) the thickness of the upper (lower) layer, and u_1 (u_2) the mean velocity in the upper (lower) layer. Integrating (2.1.1) from x=0 (location of rupture) to $x=x_f$ (time-dependent location of front), gives as an overall continuity equation for the lower layer

$$\frac{d}{dt} (\bar{\theta} a x_f) = a_0 u_0 \qquad (2.1.3)$$

where a is an equivalent pipe size given by (D is the inner diameter of the pipe)

$$a^2 = \frac{\pi}{4} D^2 \qquad (2.1.4)$$

a_0 and u_0 are defined in figure 2.1. The parameter $\bar{\theta}$,

$$\bar{\theta} = \frac{1}{a} \int_0^{x_f} a_2 (x',t) dx' \qquad (2.1.5)$$

represents the relative mean level of the interface with respect to the bottom of the pipe. This parameter is determined in section 2.2.

The equations of motion for two-layered flow may be written (4) assuming $\cos \Psi \simeq 1$,

$$\frac{\partial u_1}{\partial t} + u_1 \frac{\partial u_1}{\partial x} + \frac{1}{\rho_1} \frac{dp_0}{dx} + \frac{C_1 s_0 - s_1}{\rho_1 a_1} = gI \qquad (2.1.6)$$

and

$$\frac{\partial u_2}{\partial t} + u_2 \frac{\partial u_2}{\partial x} + \frac{1}{\rho_2} \frac{dp_0}{dx} - (1 - \frac{\rho_1}{\rho_2}) g \frac{\partial a_1}{\partial x} - \frac{2\sigma \cos \phi}{\rho_2 a_2 a} (\frac{\partial a_2}{\partial x} - I) +$$

$$+ \frac{s_1 - C_2 s_2}{\rho_2 a_2} = gI \qquad (2.1.7)$$

where σ is the interfacial tension, ϕ the contact angle, and s_0, s_1 and s_2 are shear stresses at the wall (upper layer), interface, and wall (lower layer). The interfacial-tension term is explained in the appendix. The coefficient C_1 and C_2 representing the influence of side-wall friction are given by

$$C_1 = \frac{a+2a_1}{a} \quad \text{and} \quad C_2 = \frac{a+2a_2}{a} \qquad (2.1.8)$$

The pressure p_0 at the top of the pipe cross-section is given by

$$p_0 = \rho_1 g I x + \text{constant}$$

where $I = \tan \psi$ (figure 2.1) is the slope of the pipeline.

Purely internal (exchange) flow can be separated from (2.1.6) and (2.1.7) by subtracting (4) to give

$$\frac{\partial}{\partial t} (u_1 - u_2) + \tfrac{1}{2} \frac{\partial}{\partial x} (u_1^2 - u_2^2) + \varepsilon g I + \varepsilon g \frac{\partial a_1}{\partial x} +$$

$$+ \frac{2\sigma \cos \phi}{\rho_2 a_2 a} (\frac{\partial a_2}{\partial x} - I) + \frac{C_1 s_0 - s_1}{\rho_1 a_1} - \frac{s_1 - C_2 s_2}{\rho_2 a_2} = 0 \qquad (2.1.9)$$

where

$$\varepsilon = \frac{\rho_2 - \rho_1}{\rho_2} \tag{2.1.10}$$

is the relative density difference. Integrating (2.1.9) from $x=0$ to $x=\bar{x}_f$, neglecting a possible (small) entrance pressure-loss, and approximating in the interfacial-tension term gives

$$\int_0^{\bar{x}_f} \frac{\partial}{\partial t}(u_1 - u_2)dx + \tfrac{1}{2}(u_1^2 - u_2^2)\Big|_{x=\bar{x}_f} - \tfrac{1}{2}(u_1^2 - u_2^2)\Big|_{x=0} +$$

$$+ \varepsilon g I x_f + \varepsilon g(a - a_0 - a_f) - \frac{2\sigma \cos\phi}{\rho_2 a}\left(1 + \frac{Ix_f}{a - a_0 - a_f}\right)\ln\frac{a - a_0}{a_f} +$$

$$+ \int_0^{x_f}\left(\frac{C_1 s_0 - s_1}{\rho_1 a_1} - \frac{s_1 - C_2 s_2}{\rho_2 a_2}\right)dx = 0 \tag{2.1.11}$$

where $a_f = a_2(\bar{x}_f, t)$ is the height of the front. The first three terms of (2.1.11) represent the inertia of the fluid. These terms can be shown to be approximately proportional to $\varepsilon g a_0$ or $\varepsilon g a_f$. Since the proportionality constants are not widely different and inertia is of secondary importance anyhow, it is assumed for simplicity that these terms are proportional to $\varepsilon g(a_0 + a_f)$. Equation (2.1.11) then becomes

$$\varepsilon g\left[Ix_f + a - \alpha(a_0 + a_f)\right] - \frac{2\sigma \cos\phi}{\rho_2 a}\left(1 + \frac{Ix_f}{a - a_0 - a_f}\right)\ln\frac{a - a_0}{a_f} +$$

$$+ \int_0^{x_f}\left(\frac{C_1 s_0 - s_1}{\rho_1 a_1} - \frac{s_1 - C_2 s_2}{\rho_2 a_2}\right)dx = 0 \tag{2.1.12}$$

The coefficient $\alpha(\alpha > 1)$ representing the influence of inertia is determined in section 2.4.

The friction term in (2.1.12) is determined by analyzing the laminar two-layer flow between top and bottom of the pipe (figure 2.2). The influence of the side-walls is represented by the coefficients C_1 and C_2 only (this approach is found to result in an error of about five percent for a pipe with a single, homogeneous fluid). Turbulence in the lower (water) layer is considered in section 2.5. The velocity distributions in the two layers are given by

$$u = A_1 (a - z) + B_1 (a - z)^2 \qquad (2.1.13)$$

and

$$u = A_2 z + B_2 z^2 \qquad (2.1.14)$$

where z is a coordinate normal to the pipe axis (z=0 at the bottom of the pipe). The constants A_1, B_1, A_2 and B_2 follow from expressions for the mean velocities u_1 and u_2, and the continuity of velocity and shear stress at the interface ($z=a_2$). This gives

$$\tfrac{1}{2} A_1 a_1 + \frac{1}{3} B_1 a_1^2 = u_1$$

$$\tfrac{1}{2} A_2 a_2 + \frac{1}{3} B_2 a_2^2 = u_2$$

$$A_1 a_1 + B_1 a_1^2 = A_2 a_2 + B_2 a_2^2$$

$$\rho_1 \nu_1 (A_1 + 2B_1 a_1) + \rho_2 \nu_2 (A_2 + 2B_2 a_2) = 0$$

where ν_1 and ν_2 are the kinematic viscosities of oil and water. The shear stresses s_0, s_1 and s_2 are given by

$$s_0 = \rho_1 \nu_1 A_1, \quad s_1 = \rho_1 \nu_1 (A_1 + 2B_1 a_1) = -\rho_2 \nu_2 (A_2 + 2B_2 a_2), \quad s_2 = -\rho_2 \nu_2 A_2$$

After a lengthy but straightforward calculation and assuming that $\rho_2 \approx \rho_1$, the friction term is found to be

$$\frac{C_1 s_0 - s_1}{\rho_1 a_1} \cdot \frac{s_1 - C_2 s_2}{\rho_2 a_2} \simeq -3 \frac{a_0 u_0}{a^3} \times$$

$$\times \frac{C_1 \theta^4 \nu_1^2 + \theta(1-\theta)\left[C_1\theta(1+\theta) + 2 + C_2(1-\theta)(2-\theta)\right]\nu_1\nu_2 + C_2(1-\theta)^4\nu_2^2}{\theta^3(1-\theta)^3\left[\theta\nu_1 + (1-\theta)\nu_2\right]} \qquad (2.1.15)$$

where $\theta = a_2/a$ and (see (2.1.8))

$C_1 = 3 - 2\theta$ and $C_2 = 1 + 2\theta$

2.2. Minimal friction

Equation (2.1.15) shows that the friction term tends to infinity for $\theta \to 0$ and for $\theta \to 1$, as could be expected on physical grounds. A value of θ therefore exists for which the friction term is minimal (at fixed flow rate $a_0 u_0$). This value of θ, which depends on the ratio of ν_2 to ν_1 only (figure 2.3), will be adopted since the physically correct value could be obtained only by solving the full equations (2.1.1) and (2.1.9). In this way the influence of friction is underestimated to some extent so that a conservative estimate of the leak rate is obtained.

The leak rate is not very sensitive to variations in θ. Increasing θ by ten percent resulted in an increase of about four percent in the leak rate calculated for the model pipeline described in section 3.1.

Equation (2.1.5) shows that $\overline{\theta} = \theta$, since θ does not depend on x.

2.3. Front of intruding water layer

The "head" at $x = x_f$ of the intruding water layer is conceived of as a discontinuity. Preliminary calculations showed that the height a_f of this front remains rather small (with respect to the equivalent pipe size a) under a wide range of conditions. In the absence of interfacial tension the celerity c_f of such weak fronts (e.g., $a_f < 0.3\ a$) can be approximated by (1)

$$c_f = \frac{dx_f}{dt} \simeq \sqrt{\frac{2}{1+\beta} \varepsilon g a_f} \qquad (2.3.1)$$

where β is a loss coefficient, $\beta = 0$ in the absence of losses and $\beta \sim 1$ for flow along a bottom in the case of lock-exchange flow. The leak rate was found to be insensitive to variations in β within this range.

For stronger fronts a maximum celerity exists. The maximum flow rate is almost independent of β and is given by (1)

$$a_f c_f \simeq 0.19\, a \sqrt{\varepsilon g a} \qquad (2.3.2)$$

Interfacial tension will reduce the celerity, if the contact angle ϕ is less than π (figure 2.4). Simple hydrostatics show that a stationary front can exist if

$$\tfrac{1}{2} \varepsilon \rho_2 g a_f^2 \leq (1 + \cos \phi)\, \sigma \qquad (2.3.3)$$

Using (2.3.3) equation (2.3.1) can be modified for interfacial tension to give

$$c_f \simeq \sqrt{\frac{2}{1+\beta} \varepsilon g a_f \left[1 - \frac{2(1 + \cos \phi)}{\varepsilon g a_f^2} \frac{\sigma}{\rho_2}\right]} \qquad (2.3.4)$$

2.4. Flow at rupture

The oil is assumed to flow out freely at the rupture. As a consequence, the flow at the rupture is internally critical. The condition for critical flow is

$$\frac{u_1^2}{\varepsilon g a_1} + \frac{u_2^2}{\varepsilon g a_2} = \frac{u_0^2}{\varepsilon g a_0} \left[1 + \left(\frac{a_0}{a - a_0}\right)^3\right] = 1 \qquad (2.4.1)$$

The coefficient α introduced in (2.1.12) to account for the inertia of the fluid, can be determined in the following way. Neglecting interfacial tension, equation (2.1.12) gives for small times (inertia then controls the flow, and the flow rates are maximal)

$$a_0 + a_f \simeq \frac{a}{\alpha} \tag{2.4.2}$$

Equations (2.3.1) and (2.3.2) give

$$a_f \simeq (0.19 \sqrt{\frac{1+\beta}{2}})^{2/3} a \tag{2.4.3}$$

Equations (2.3.2) and (2.4.1), together with the continuity condition $a_0 u_0 = a_f c_f$ give

$$a_0 \simeq (0.19)^{2/3} a \tag{2.4.4}$$

Substituting from (2.4.3) and (2.4.4), equation (2.4.2) gives

$$\alpha \simeq \frac{3.0}{1+(\frac{1+\beta}{2})^{1/3}} \tag{2.4.5}$$

This value agrees with a more direct estimation of the inertia terms in (2.1.11).

The condition for critical flow, equation (2.4.1), sets an upper bound to the leak rate. The leak rate Q would be maximal when $a_0 = \frac{1}{2} a$, and would then amount to

$$Q = 0.25\ a^2 \sqrt{\varepsilon\ g\ a} \tag{2.4.6}$$

The flow at the rupture would then be double-critical. However, the intrusion process also sets an upper bound to the leak rate. According to (2.3.2) this maximum is given by

$$Q = 0.19\ a^2 \sqrt{\varepsilon\ g\ a} \tag{2.4.7}$$

The coefficient in the latter expression is smaller and therefore (2.4.7) represents the real maximum.

The inflow of water at the simulated rupture in the model pipeline (section 3) was of Borda-type, so that contraction of the inflow then should be taken into account. Fixing the coefficient of contraction at 1/2, the maximum leak rate can now be estimated from the condition (figure 2.5)

$$\frac{Q^2}{\varepsilon g a_0^3 a^2} + \frac{Q^2}{\varepsilon g (\frac{a-a_0}{\sqrt{2}})^3 (\frac{a}{\sqrt{2}})^2} = 1 \qquad (2.4.8)$$

The maximum leak rate occurs when $a_0 \approx 0.39\ a$ and amounts to

$$Q \approx 0.15\ a^2 \sqrt{\varepsilon\ g\ a} \qquad (2.4.9)$$

In this case the real maximum is given by (2.4.9); the flow at the rupture then is double-critical.

Prescribing either (2.4.7) or (2.4.9) as the controlling leak rate was found to be of secondary importance for the theoretical results to be discussed in sections 4 and 5.

The volume V of leaked oil is given by

$$V(t) = \int_0^t Q(t')dt' = \bar{\theta} a^2 x_f \qquad (2.4.10)$$

where Q is given by either (2.4.7) or (2.4.9) when inertia is controlling the flow, and by (see (2.1.3))

$$Q = a\ a_0\ u_0 \qquad (2.4.11)$$

in later stages when friction is dominating.

2.5. Turbulence in water layer

Under prototype conditions, but also in relatively large model pipelines, the flow of the water layer can become turbulent* during a

---

*Possible turbulence in the oil layer is not considered here.

certain initial phase of the exchange process. Turbulence in this layer is accounted for by replacing in (2.1.15) the viscosity ν_2 by an effective viscosity ν_t when the Reynolds number defined as

$$Re = \frac{u_2 a_2}{\nu_2} = \theta \frac{a c_f}{\nu_2} \tag{2.5.1}$$

is larger than a critical value assumed to be 2400 (5). The effective viscosity is determined by requiring that the shear stress at the wall when computed using ν_t be equal to the actual, turbulent shear stress. This gives, for flow between two parallel plates,

$$6 \nu_t \frac{u_2}{a_2} = u_*^2 \tag{2.5.2}$$

where u_* is the friction velocity. Blasius'law for smooth walls is used to express u_* as a function of u_2 to give (5, p. 575)

$$u_*^2 \simeq \frac{0.037}{Re^{\frac{1}{4}}} u_2^2 \tag{2.5.3}$$

Substituting from (2.5.1) and (2.5.3) the effective viscosity given by (2.5.2) becomes

$$\nu_t = \begin{cases} 0.0062\ Re^{3/4}\ \nu_2 & , \quad Re > 2400 \\ \nu_2 & , \quad Re < 2400 \end{cases} \tag{2.5.4}$$

Since Re depends on time, ν_t also becomes a function of time. Figure 2.3 shows that, strictly speaking, the parameter θ then also should become a function of time. However, this parameter was kept constant in the computations.

3. Experiments

3.1. Experimental set-up

Experiments were carried out in a horizontal PVC model pipeline,*

---

* Experiments with a sloping pipeline are planned for the near future.

total length 100.30 m and inner diameter 0.103 m. The diameter was chosen so that the influence of interfacial tension was small; the length was determined by the requirement that friction should be dominating in later stages of the exchange process. Transparent sections, length 0.90 m, were inserted at x = 13, 26, 39, 52, 65, 78, 91 and 97.80 - 100.30 m. A large-radius bend was constructed at x = 19.60 m. One end of the pipe was closed with a plastic plate; the other (open) end simulating the rupture was inserted in a steel reservoir, cross-section about 0.53 x 1.00 m^2 (inner area 0.534 m^2) and height 2.00 m (figure 3.1). This reservoir served to supply the pipe with oil and fresh water. A spring-loaded valve used to close the open end was installed on the bottom of the reservoir. The reservoir had windows for observing the outflow of oil from the pipe and the level of the interface between water and oil. This level could also be read using a submerged float that followed the interface. Since the outflow of oil from the pipe initially causes large disturbances at the interface, a perforated steel screen sheltering the float was placed vertically in the reservoir.

The pipeline was filled with oil through a hose connecting the reservoir and a tapping, diameter 18 mm, at the lower side of the pipe. After an experiment had been finished, the oil and water in the pipe were supplied to a separating tank through the same tapping.

The oil used was a mixture of common fuel oil and, to increase the viscosity, a more viscous oil (Tellus, Shell). The viscosity of the mixture was about 10^{-5} m^2/s, but a marked temperature dependence was observed (figure 3.2). The temperature varied somewhat during an experiment and also along the pipeline. The viscosity of the oil therefore also varied somewhat.

In order to check the reproduceability three experiments were done. The data relating to these experiments are given in table 3.1. The mixing ratio of the oils in experiments nos. 2 and 3 slightly differed from that in experiment no. 1. The interfacial tension was determined by measuring the maximal height (about 7 mm) of a submerged water drop, as shown in figure 2.4.

exp. no.	1	2	3
ρ_1 (kg/m^3)	844	847	847
ρ_2 (kg/m^3)	999	999	999
ε	0.155	0.152	0.152
temperature (^{o}C)	17.8-18.7	17.4-18.2	17.5-18.6
$\nu_1 \times 10^6$ (m^2/s)	10.1-10.4	9.9-10.4	9.6-10.3
$\nu_2 \times 10^6$ (m^2/s)	1.05	1.06	1.05
σ (N/m)	0.018	0.018	0.018
ϕ	0	0	0

Table 3.1. Experimental data.

3.2 Scaling laws

The scale factor n_Φ for a quantity Φ is defined as

$$n_\Phi = \frac{\Phi \text{ prototype}}{\Phi \text{ model}} \qquad (3.1.1)$$

The theory of section 2 suggests that, apart from geometrical similarity, the following scaling laws should be observed (also see (3))

- internal Froude number : $\dfrac{n_u^2}{n_\varepsilon n_l} = 1$
- Reynolds number
  - oil layer : $\dfrac{n_u n_l}{n_{\nu_1}} = 1$
  - water layer : $\dfrac{n_u n_l}{n_{\nu_2}} = 1$
- time : $\dfrac{n_t n_u}{n_l} = 1$

Here n_l is the length scale. These relations give

$$n_{\nu_1} = n_{\nu_2} = n_l \sqrt{n_\varepsilon n_l} \qquad (3.1.2)$$

and

$$n_t = \sqrt{\frac{n_1}{n_\varepsilon}} \tag{3.1.3}$$

The scale factor of the volume of leaked oil is given by

$$n_V = n_1^3 \tag{3.1.4}$$

Table 3.2 gives the various scale factors and required viscosities of the model oil. The prototype data concerning the pipeline from the Q - 1 block to the Dutch shore were adopted from (3).

The required viscosity of the lower layer is not shown, since, as in the prototype, water was the intruding fluid. The flow in the water layer in the model pipeline was laminar, except, possibly during some

	prototype	exp.no.1	exp. nos.2 and 3
D (m)	0.48	0.103	0.103
ρ_1 (kg/m^3)	930	844	847
ρ_2 (kg/m^3)	1025	999	999
n_1	-	4.66	4.66
n_ε	-	0.601	0.613
n_{ν_1}	-	7.80	7.87
n_t	-	2.79	2.76
n_V	-	101	101
$\nu_1 \times 10^6$ (m^2/s)	75	9.62	9.53

Table 3.2. Scale factors, prototype and model quantities.

tens of seconds following the start of an experiment, whereas it will be turbulent in the prototype pipeline. Since n_{ν_2} = 7.80 to 7.87, the model viscosity $\nu_2 = 1.05 \times 10^{-6}$ m^2/s therefore is equivalent to an effective prototype viscosity $\nu_t \simeq 8.3 \times 10^{-6}$ m^2/s. This point will be reconsidered in section 5.

The actual viscosity of the oil mixture was somewhat greater than required, the temperatures during the experiments being lower (by about 0.5^{o}C) than expected.

3.3. Experimental procedure

The model pipeline was filled with oil from the reservoir through the filling hose (figure 3.1), while the spring-loaded valve was closed. The pipe was placed under an angle to remove entrapped air. When all the air had been driven out, the pipe was placed back in the horizontal position, and the valve in the filling hose was closed. The oil remaining in the reservoir was then supplemented with water from the laboratory water supply system until the reservoir was completely filled. Next the initial position of the float was read.

An experiment was started by opening the spring-loaded valve. The level of the float was read at regular time-intervals, and the passage of the intruding water front at the transparent sections was timed. In experiment no. 1 the readings of the float were checked with (less accurate) observations of the interface through the windows. In experiment no. 3 the thickness of the water layer at $x = 12.80$ m was also measured using a water box to reduce the refraction of light at the pipe wall. The total measuring time was about two hours, which is about three times the travelling time the front needed to reach the end of the pipe.

After an experiment had been finished the oil in the pipe was allowed to keep on flowing back into the reservoir overnight. Next the spring-loaded valve was closed, and the water and oil then still present in the pipe were supplied to the separating tank. The separated oil was pumped back into the reservoir.

4. Experimental and theoretical results

When the spring-loaded valve was opened, oil started to flow out at the top of the cross-section simulating the rupture. Simultaneously water from the reservoir started to flow in at the lower part. The oil streamed out as a connected plume, and oil drops did not form until the plume had risen above the pipe. This indicates that the outflow of oil was not hindered by interfacial-tension effects. The thickness of the plume and the leak rate decreased as time elapsed. A sharp interface between oil and water developed in the pipe as well as in the reservoir. Observations at the transparent sections indicated that the flow in the pipe was laminar, except possibly during the time that the front had not yet reached the first transparent section (at

x = 13 m). The theoretical result indicates turbulent flow during about 130 s ($x_f \leq 12$ m), and laminar flow afterwards.

According to theory interfacial tension has only a small influence on the results: neglecting interfacial tension increases the calculated leak rate by about six percent.

4.1. Volume of leaked oil

The experimental volume V of leaked oil is shown in figure 4.1 together with a theoretical prediction. Prototype scales calculated using the scale factors given in table 3.2 are indicated, as well as the instants at which the front reached the end of the pipe ($x_f = L$). The experiments indicate that the reproduceability is good. Initially the theoretical and experimental leak rates (= dV/dt) are as predicted by (2.4.9), but afterwards friction gradually reduces the leak rates. Remarkably, the reflection of the front from the end of the pipe seems to have no observable influence on the leak rate during the measuring period (the calculated travelling time of the reflected internal wave is about 270 s). Damping of the reflected wave by friction (see below) may explain this finding. The theoretical result (dash-dot curve) applies to the model pipeline; the dashed curve is for a pipe so long that the front does not reach the end within the period shown.

The theoretical volume of leaked oil is somewhat larger than observed, in accord with the assumption of minimal friction (section 2.2). Nevertheless the agreement between experimental and theoretical results is satisfactory, even after the front has reached the end of the pipe.

4.2. Location of front

The observed and calculated locations of the front are shown in figure 4.2. The celerity of the front decreases as its height decreases in course of time. Initially the experimental celerity is larger than the theoretical one, but in later stages the celerities agree quite well. After the front had reflected from the end of the pipe, an internal wave started to travel back. Presumably owing to friction, however, this wave became indiscernable after having travelled less than 2 m.

Figure 4.3 shows the volume of leaked oil versus the location of

the front. The experiments indicate a linear relationship, which is rather surprising since different mechanisms are dominating at small and large times (inertia and friction, respectively). The linear relationship may therefore be coincidental. The experiments indicate that, on the average, 37 to 38 percent of the pipe (section between rupture and front) is filled with water. The theoretical result (figure 2.3) is about 43 percent.

4.3. Thickness of water layer

Figure 4.4 shows the thickness of the water layer at x = 12.80 m observed during experiment no. 3 as a function of time. The height of the front passing after about 90 s was less than 20 mm. An accurate measurement was not possible because of turbulence and temporary mixing of oil and water at the front. The theoretical height of the front at x = 12.80 m is about 9 mm. After passage of the front the flow quickly becomes laminar.

As in figure 4.1, no influence of wave reflection from the end of the pipe seems noticeable in figure 4.4.

The observed linear relationship between V and x_f (figure 4.3) suggests that the thickness a_2 of the water layer, which in general is a function of x and t, may be approximated by a function of $x/x_f(t)$ alone during the period that the front has not yet reached the end of the pipe. As shown in figure 4.5, the relation between a_2 and x/x_f is more or less linear.

4.4. Simulation of RJBA model experiment

An experiment similar to that described here was carried out by R.J.Brown & Associates (hereafter RJBA) (3), though on a much smaller scale. The inner diameter of the (horizontal) pipe was 16 mm and the length 3.00 m. The density of the oil (in fact a mixture of gasoline and oil) was 750 kg/m^3, its kinematic viscosity was 0.74×10^{-6} m^2/s. The intruding fluid was fresh water.

Interfacial tension is likely to substantially reduce the leak rate on such a small scale. Figure 4.6 shows some theoretical results together with RJBA's experimental result. As opposed to the presentation in (3), the scales indicated are model scales. This figure suggests

that interfacial tension must be taken into account to obtain lake rates of the same magnitude as observed. The drops forming at the location of rupture were photographed by RJBA. The size of these drops suggests $\sigma \sim 0.02$ N/m.

5. Theoretical results for a prototype pipeline

Calculations were carried out for the pipeline from the Q-1 block in the Dutch sector of the North Sea to IJmuiden (table 3.2). Results for various slopes of the pipeline are shown in figure 5.1. Here a volume of leaked oil equal to 62.6 m^3 corresponds with a travelling distance of the front equal to 1000 m. The leak rates increase with slope until the maximum —assumed to be given by (2.4.7) in this case — has been reached (here for $I \simeq 0.01$). Further increase of the slope would not increase the leak rate.

RJBA (3) extrapolate their experimental results in an apparently arbitrary way to give a maximum volume of leaked oil of 20 m^3 for a horizontal pipeline. The present result shows that even for a horizontal pipeline the volume of oil released continues to increase, thereby attaining values much larger than 20 m^3.

According to the calculations the flow in the water layer is always turbulent when $I \geq 0$. In the case of the horizontal pipeline the effective viscosity calculated decreased from $\nu_t \simeq 25 \times 10^{-6}$ m^2/s for $x_f = 0$ to $\nu_t \simeq 5 \times 10^{-6}$ m^2/s for $x_f = 1000$ m (for increasing x_f the flow would eventually become laminar). As argued in section 3.2 the viscosity of the water layer in the experiments corresponds with an effective prototype viscosity of 8.3×10^{-6} m^2/s. This value is well within the range calculated, the calculation predicting that $\nu_t = 8.3 \times 10^{-6}$ m^2/s when $x_f \simeq 300$ m. The model viscosity of the water layer therefore is not unrealistic.

The theoretical results indicate a marked influence of the slope of the pipeline, and it may be questioned whether this is correct in a quantitative sense. Friction is modelled so that an upper bound to the volume of leaked oil is obtained. This approach has been shown experimentally to give results for a horizontal pipeline that are only slightly conservative. Large deviations from physically realistic values for sloping pipelines seem unlikely, since the relative contribution of friction to the momentum balance decreases as the slope

increases. Future experiments with a sloping pipe have to give decisive answers here, however.

The total volume of leaked oil (that is, the volume leaked from both sides of the idealized rupture) can be obtained by adding the results for +I and -I. Accepting the theoretical results, figure 5.1 shows, then, that the total volume of leaked oil is smallest for a horizontal pipeline, although the difference from the case with I = 0.001 is very small.

6. Conclusions

The investigation reported dealt with the exchange flow of oil and sea-water following the rupture of a submarine pipeline. Laboratory experiments in a horizontal model pipeline were carried out, and a simple mathematical model was developed, to determine the volume of leaked oil as a function of time. The following conclusions can be drawn from the results:

- A distinct two-layer flow comes into existence in the pipeline after the pipe has ruptured, the water intruding in the lower part of the pipe. Inertia initially controls the leak rate, but afterwards friction gadually reduces the leak rate in horizontal and slightly sloping pipelines. In long pipelines the volume of oil released continues to increase, however, unless a low point would eventually stop the exchange process.
- A finite length of the pipeline, or a low point, in the first instance does not noticeably decrease the leak rate. A conservative assumption is that the pipeline is infinitely long and has a constant slope.
- The length-averaged thickness of the water layer was almost independent of time in the experiments done.
- Interfacial tension substantially reduces the leak rates in small-scale models.
- The mathematical model is predictive in that no use is made of any adjustable constants. The prediction of the volume of leaked oil is slightly conservative. The results are in satisfactory agreement with the measurements.

- Calculations indicate that even small inclinations of the pipeline markedly increase the total leak rates. This result has still to be verified experimentally.

7. Acknowledgements

Part of the research reported was supported financially by Rijkswaterstaat, Directie Noordzee (Public Works Department, North Sea Direction). The author is indebted to Mr. J. Groeneveld who designed and constructed the experimental set-up, and to Mr. A.M. den Toom who carried out the numerical computations.

References

1. Kranenburg, C., "Internal fronts in a two-layer flow", J. Hydr. Div., ASCE, 104, HY10, 1978, pp. 1449-1453.
2. Mundheim, Ø. and T. Fanneløp, "Studies of oil spills from blowouts and broken underwater pipelines", Report S-III/3, Statoil and Norwegian Institute of Technology, Trondheim, 1976.
3. R.J. Brown & Associates, "Crude oil pipeline project from block Q - 1 to shore - Oil released from a ruptured submarine pipeline", Report (draft), 1981.
4. Schönfeld, J.C. and C. Kranenburg, "Density currents and internal waves" (in Dutch), Lecture notes, Department of Civil Engineering, Delft University of Technology, Delft, 1982.
5. Schlichting, H., "Boundary-layer theory", 6th ed., McGraw-Hill, 1968.

Notation

a	equivalent pipe size given by (2.1.4)
a_0	thickness of upper layer at location of rupture
a_1, a_2	thicknesses of upper and lower layers
a_f	height of front
A_1, A_2, B_1, B_2	constants
C_1, C_2	constants accounting for side-wall friction
c_f	$= dx_f/dt$, celerity of front
D	inner diameter of pipe
g	gravitational acceleration
I	$= \tan \psi$, slope of pipeline
L	length of pipeline
$n_{..}$	scale factor
p_0	pressure at top of cross-section
Q	$= dV/dt$, leak rate
Re	Reynolds number of lower layer
s_0, s_1, s_2	shear stresses
t	time
u	velocity in x-direction
u_0	velocity of oil layer at location of rupture
u_1, u_2	velocities of upper and lower layers
u_*	friction velocity
V	volume of leaked oil
x_f	coordinate of front
x, z	coordinates along pipeline and normal to it ($x = 0$ at location of rupture)
α	coefficient representing inertia of fluid
β	loss coefficient
ε	$=(\rho_2 - \rho_1)/\rho_2$, relative density difference
θ	$= a_2/a$, relative thickness of lower layer
$\bar{\theta}$	parameter defined by (2.1.5)
ν_1, ν_2	kinematic viscosities of upper and lower layers
ν_t	effective (turbulent) viscosity of lower layer
ρ_1, ρ_2	densities of upper and lower layers
σ	interfacial tension
ϕ	contact angle
ψ	angle of inclination of pipeline to the horizontal

Appendix - The interfacial-tension term in the equations of motion

The component F_1 of the interfacial tension in the plane of one of the vertical side-walls (the circular cross-section of the pipe is approximated by a square) is, see figure A1,

$$F_1 = \sigma \cos \phi$$

This force locally deforms the interface and it is directed normally to the part of the interface that is not affected by interfacial tension. The plane coinciding with this part of the interface (the dashed line in figure A1 is selected as the separation between upper and lower layers. As a consequence, a force owing to interfacial tension arises in the equation of motion for the lower (upper) layer if the contact angle ϕ is less than $\pi/2$ ($> \pi/2$). Since $\phi < \pi/2$ for oil-water, this case is considered in detail.

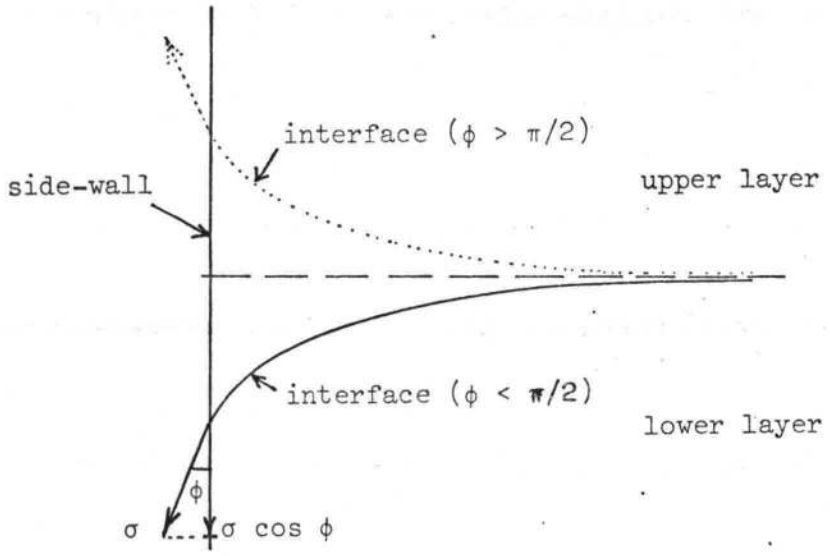

Figure A1

Some fluid of the upper layer is included in the lower layer as a result of the deformation of the interface near the side-wall. The related deficit F_2 in weight per unit length is given by, see figure A2,

$$F_2 = \sigma \cos \phi \cos (\psi - \gamma)$$

where γ is the angle between the undisturbed interface and the axis of the pipe, $\tan \gamma = \partial a_2 / \partial x$.

The net force in x-direction caused by interfacial tension consists of components of the forces F_1 and F_2. The net force F_3 in x-direction is

$$F_3 = F_1 \sin \gamma - F_2 \sin \psi$$

For small angles γ and ψ this force becomes

$$F_3 \simeq \sigma \cos \phi \left(\frac{\partial a_2}{\partial x} - I\right)$$

In equation (2.1.7) the forces are divided by $\rho_2 a_2 a$. Transferring the force term to the left-hand side gives as a contribution for two side-walls in (2.1.7)

$$- \frac{2\sigma \cos \phi}{\rho_2 a_2 a} \left(\frac{\partial a_2}{\partial x} - I\right)$$

If $\phi > \pi/2$ a term,

$$+ \frac{2\sigma \cos \phi}{\rho_1 a_1 a} \left(\frac{\partial a_1}{\partial x} + I\right)$$

would appear on the left-hand side of (2.1.6) instead of (2.1.7).

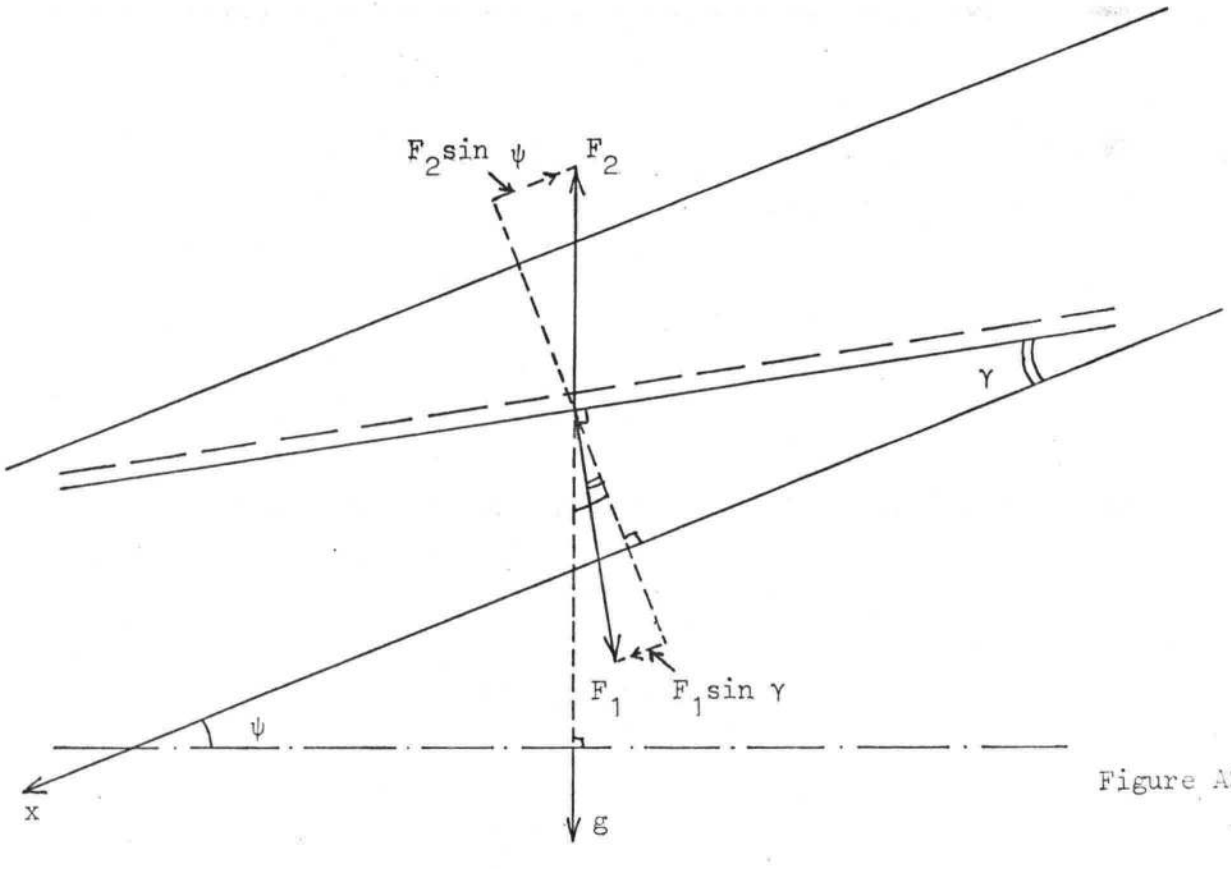

Figure A2

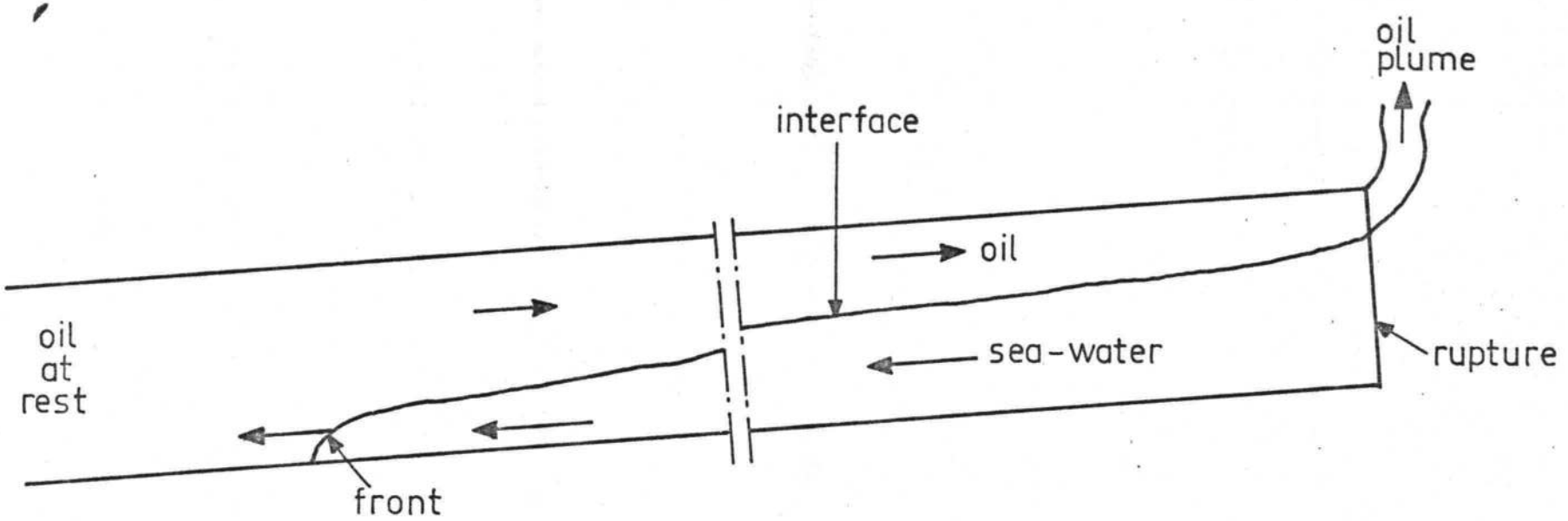

Fig. 1.1. Exchange flow of oil and sea-water.

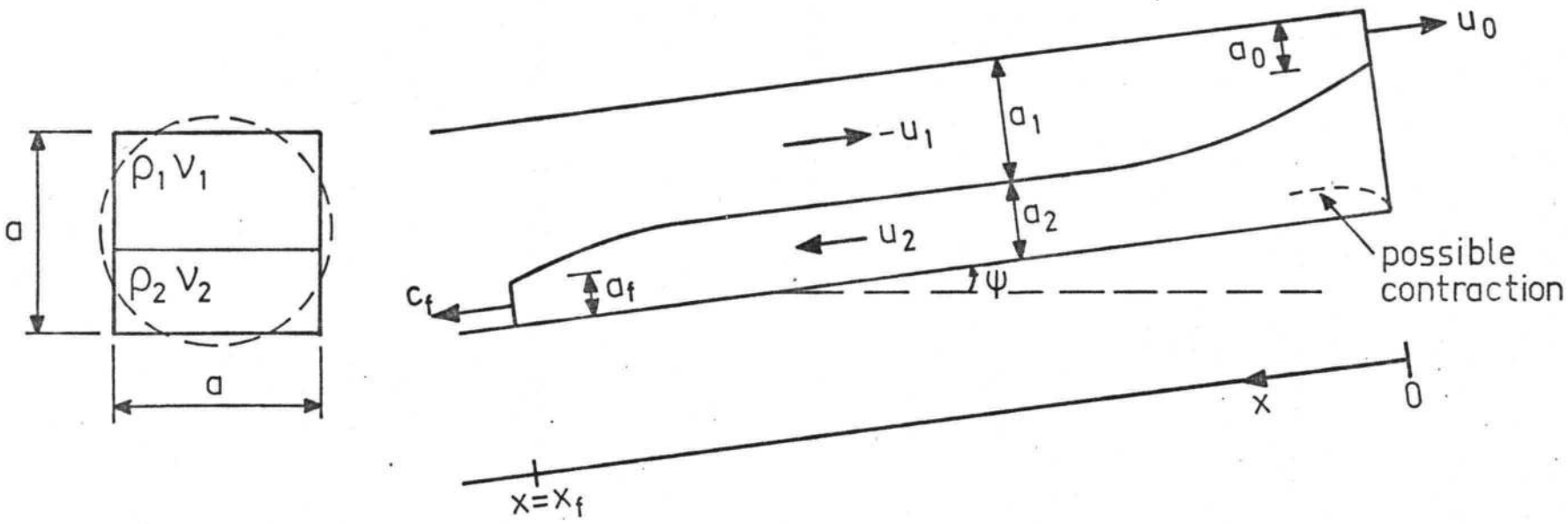

Fig. 2.1. Definition sketch.

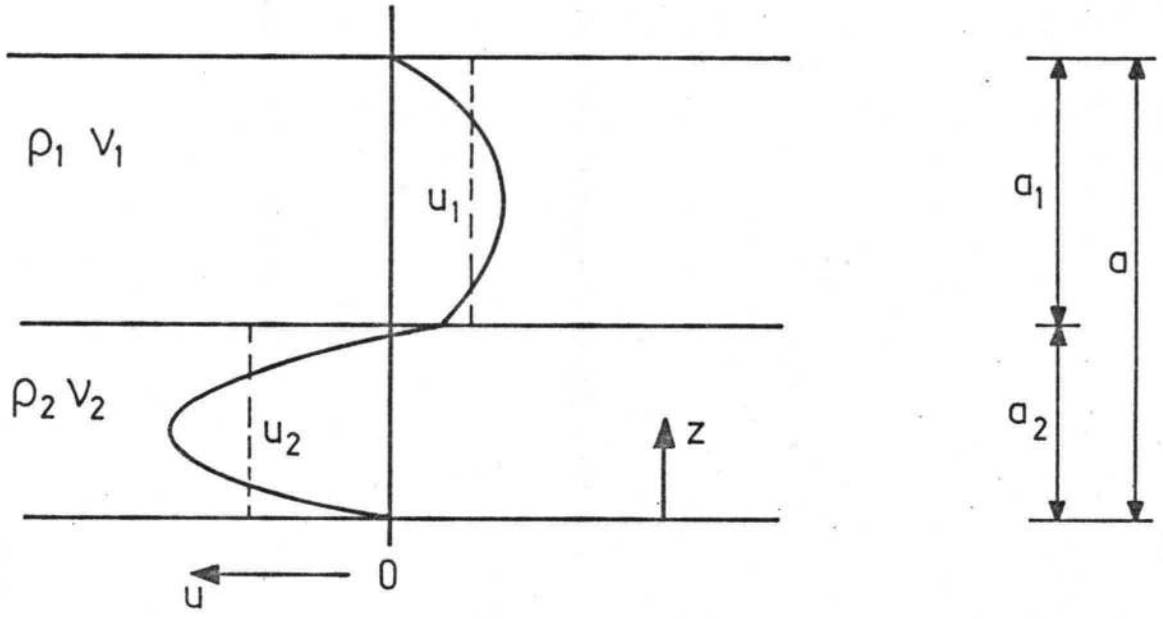

Fig.2.2. Velocity distribution (Laminar flow).

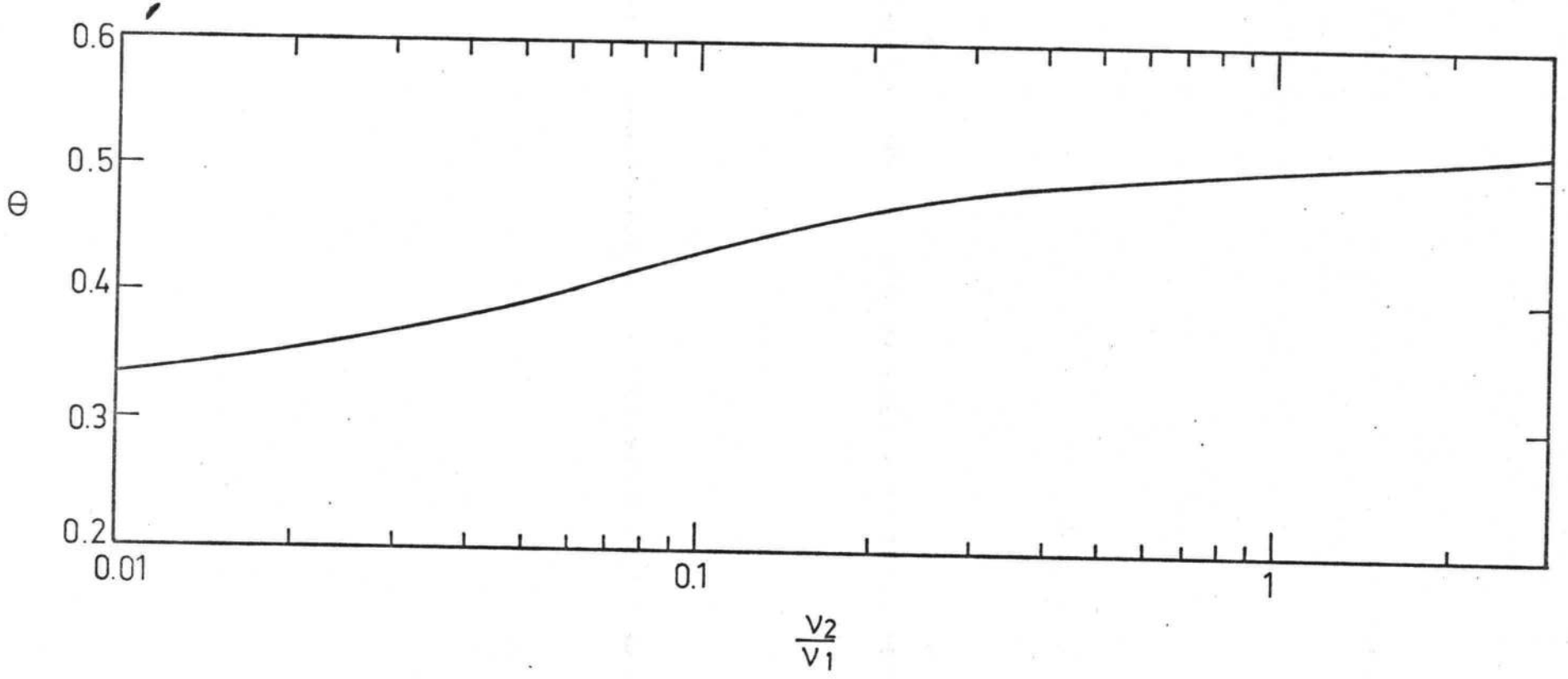

Fig. 2.3. Value of parameter Θ .

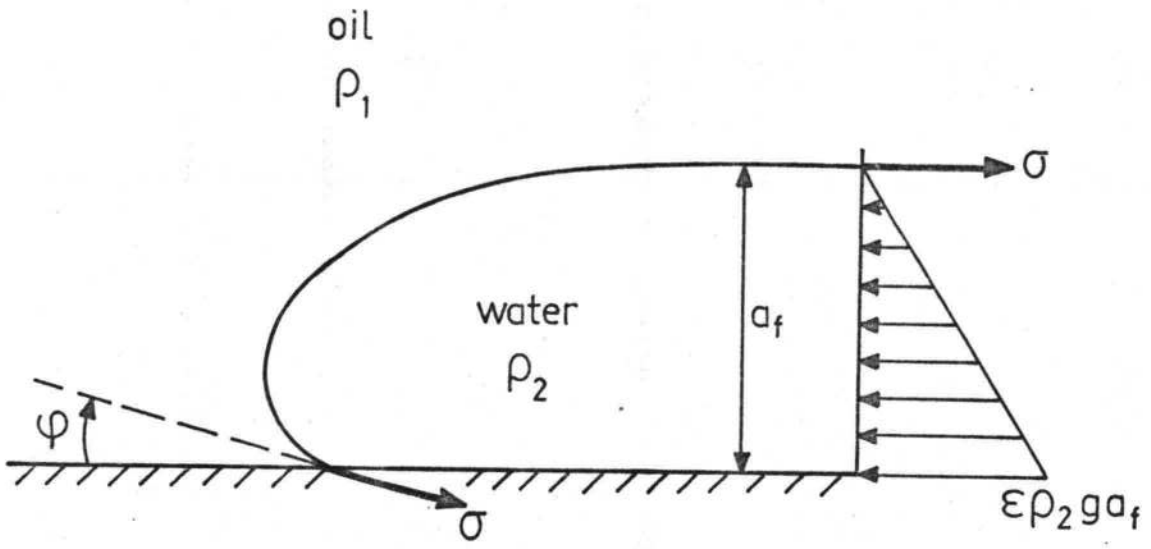

Fig. 2.4. Influence of interface tension on stationary front.

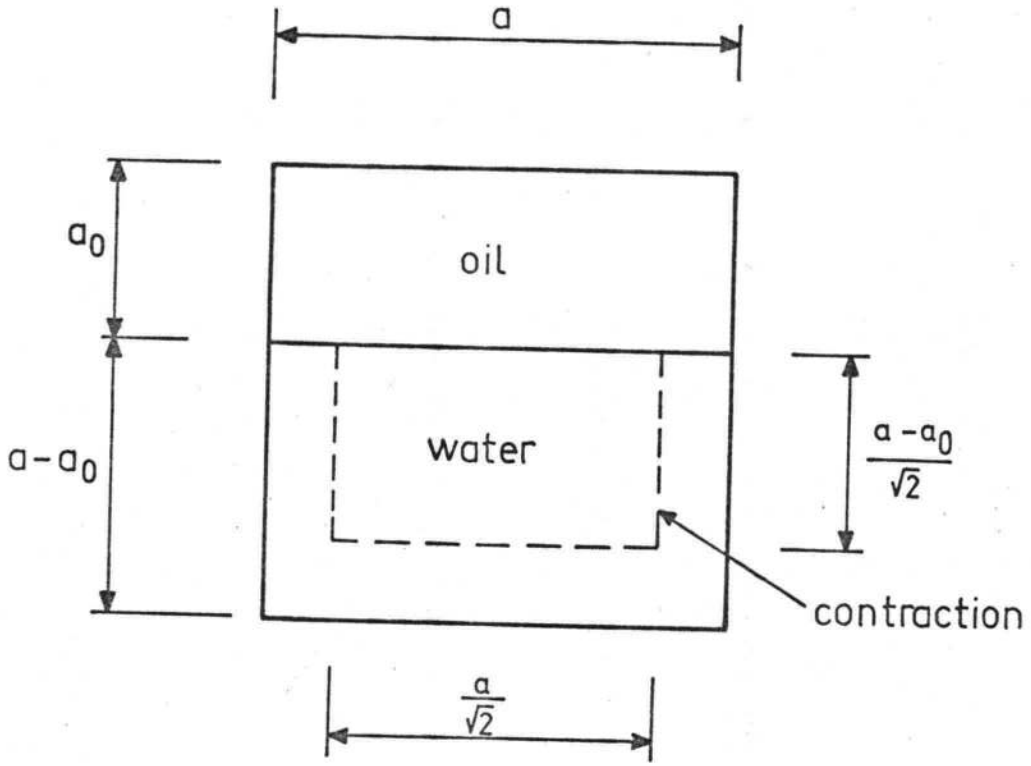

Fig. 2.5. Schematized flow at rupture.

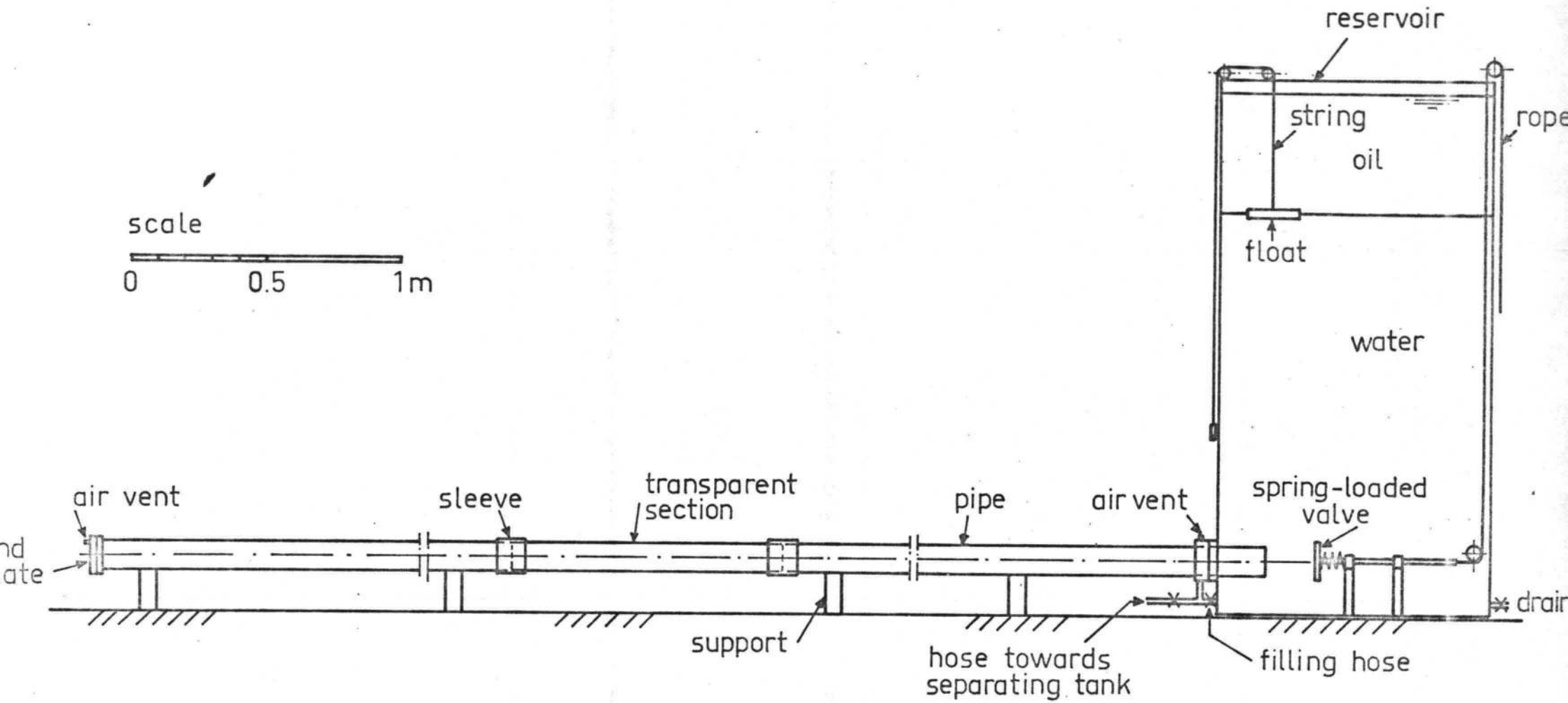

Fig. 3.1. Diagram of model pipeline .

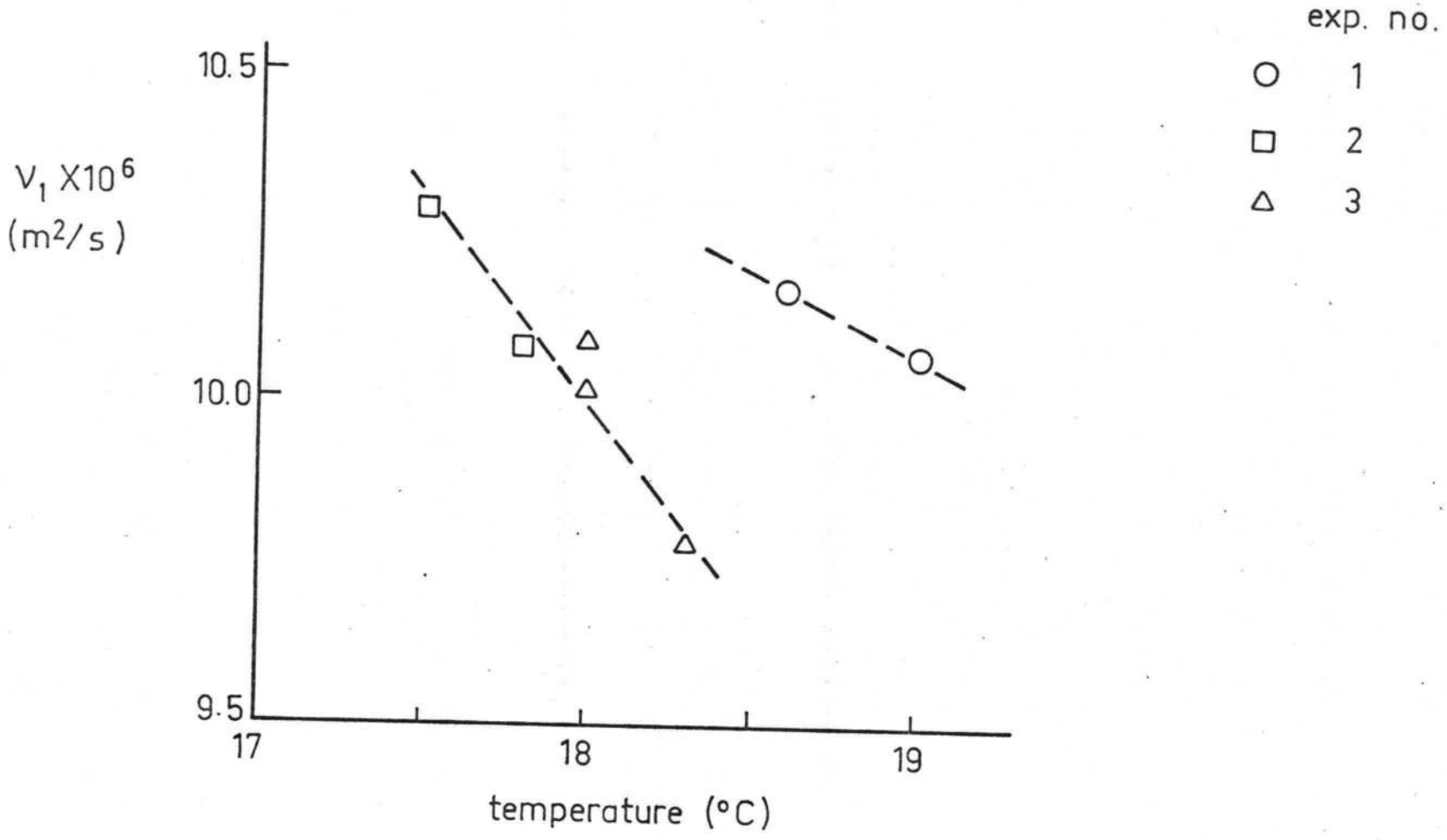

Fig. 3.2. Viscosity of oil mixture.

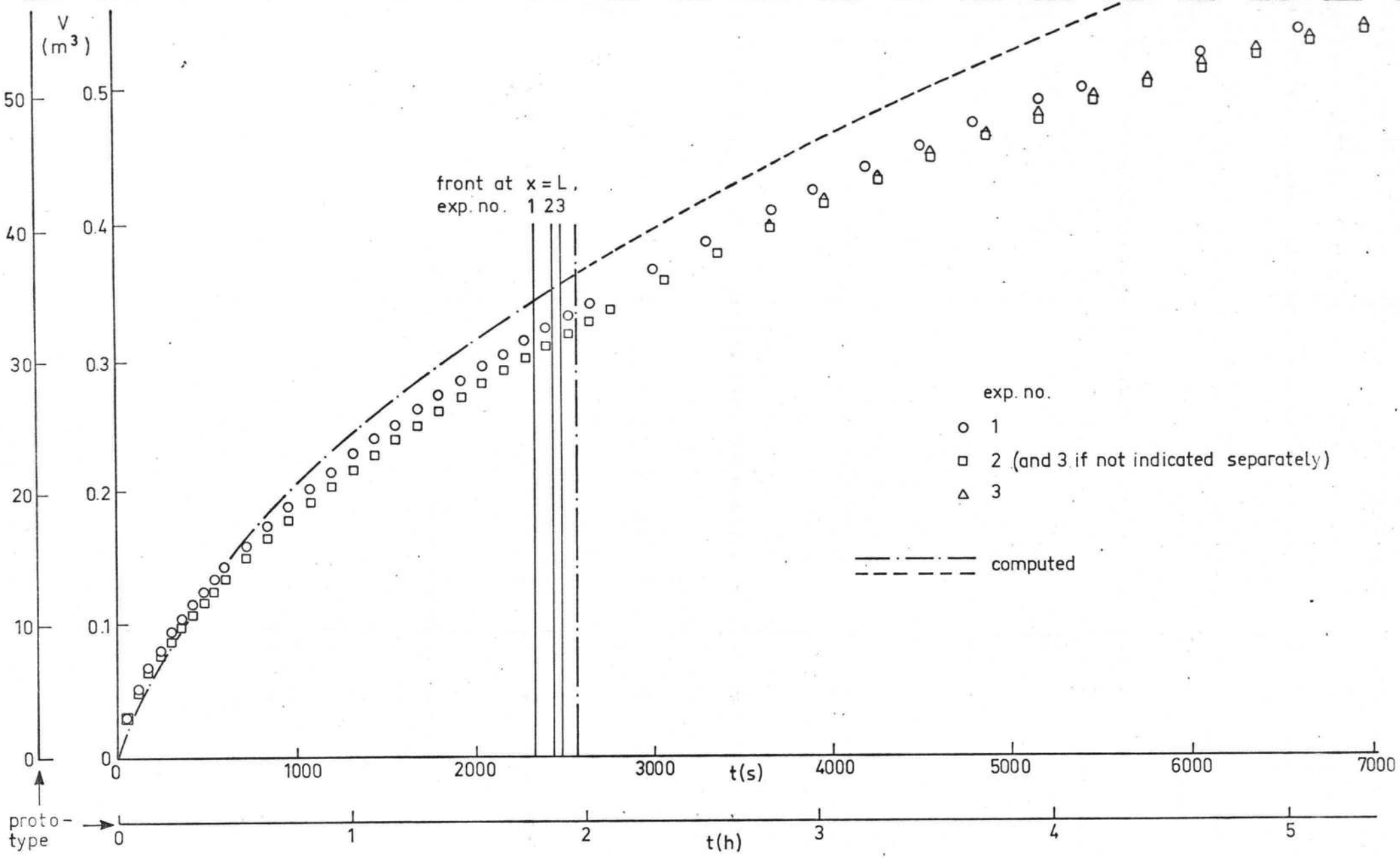

Fig. 4.1. Volume of leaked oil (model pipeline).

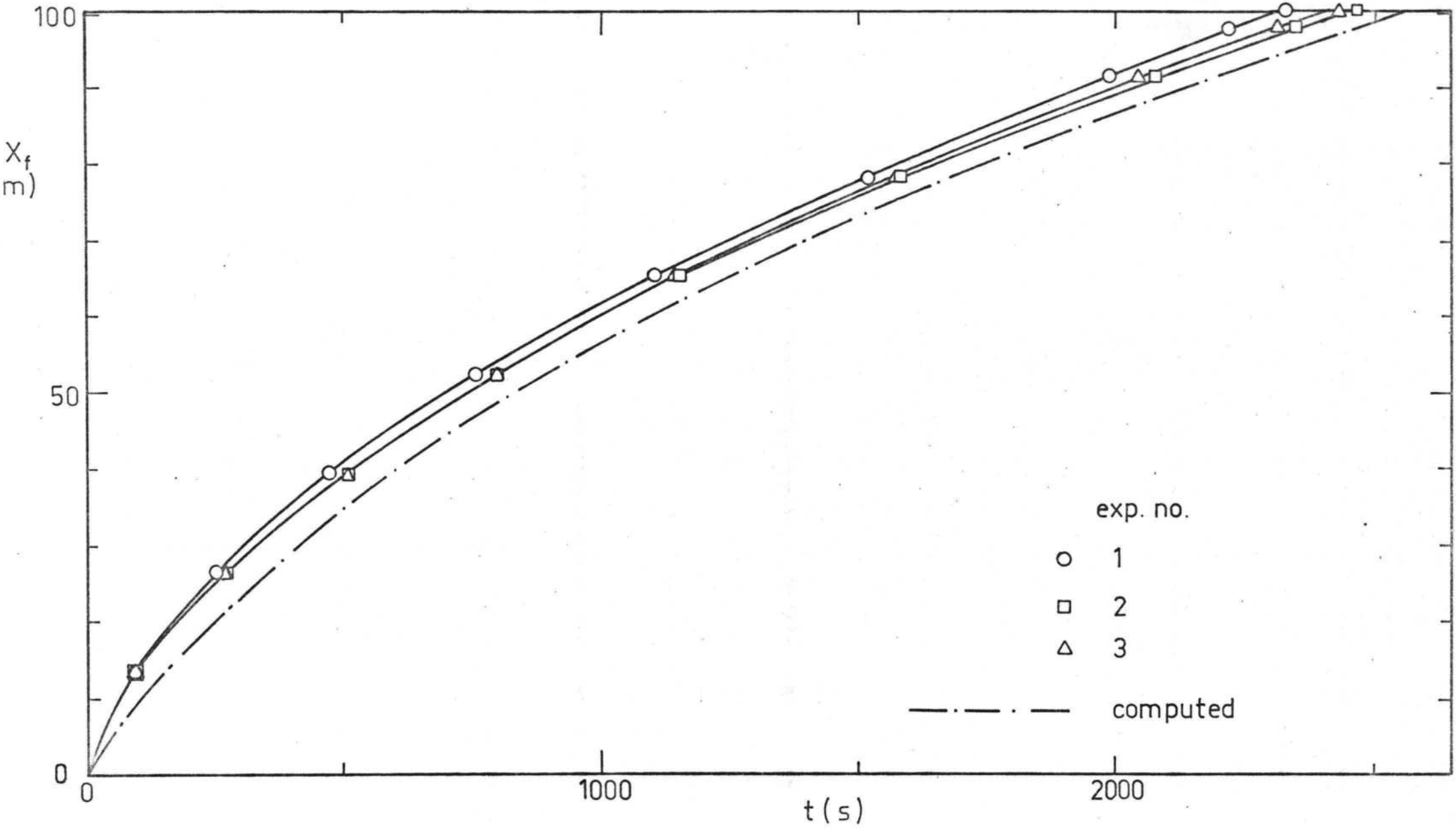

Fig. 4.2. Location of front.

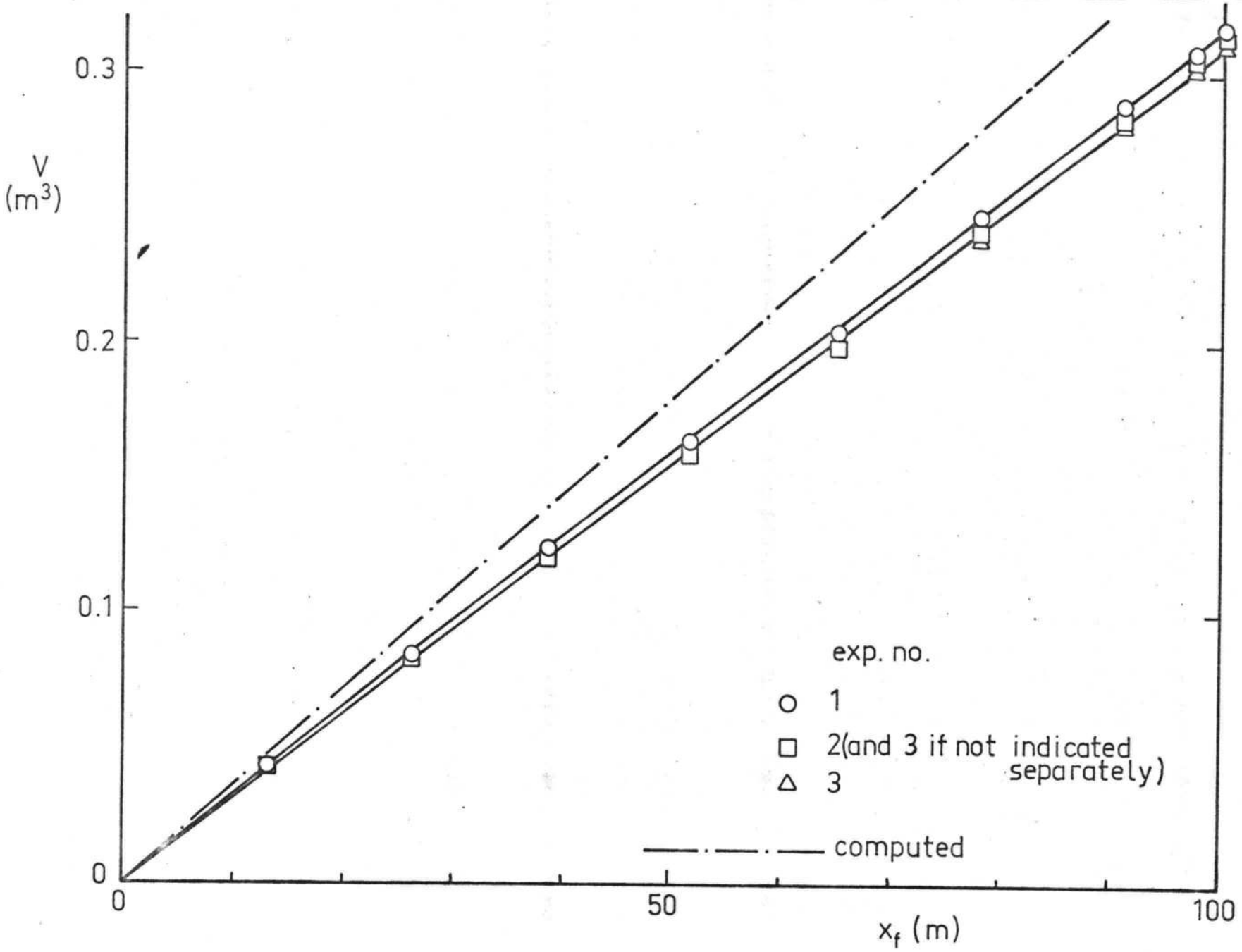

Fig. 4.3. Volume of leaked oil versus location of front.

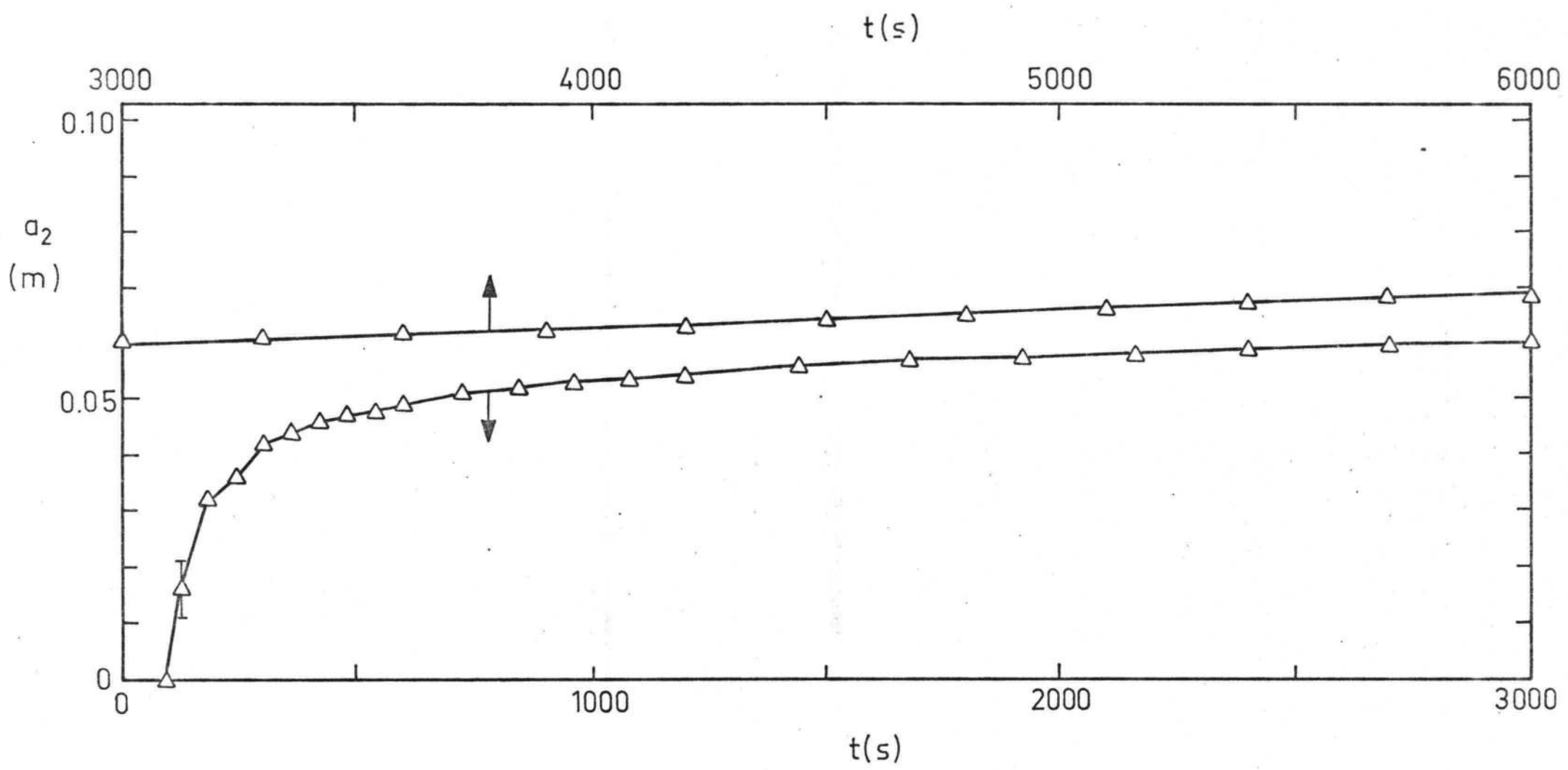

Fig.4.4. Thickness of water layer at x = 12.80 m (exp. no. 3).

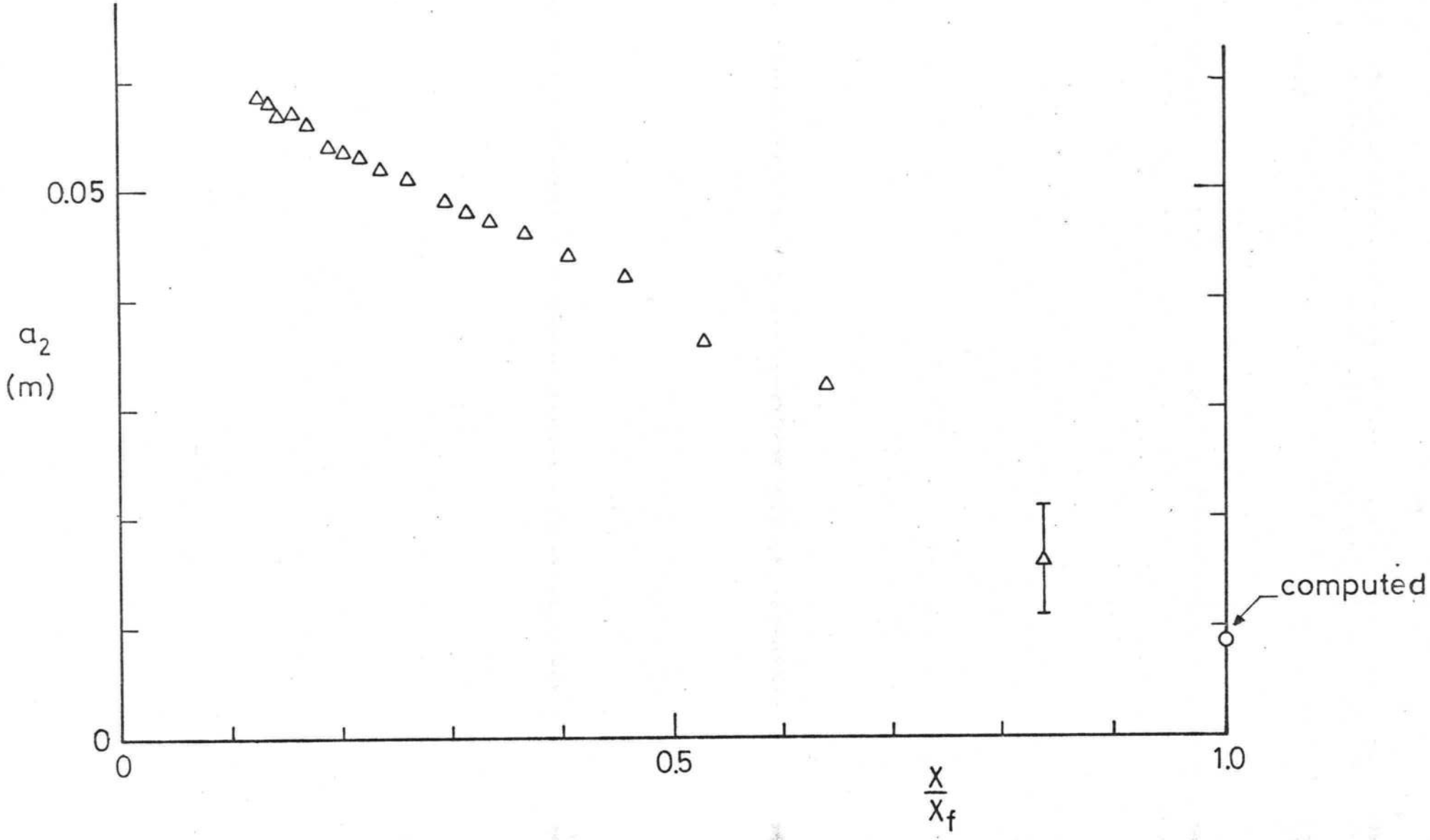

Fig. 4.5. Thickness of water layer versus x/x_f.

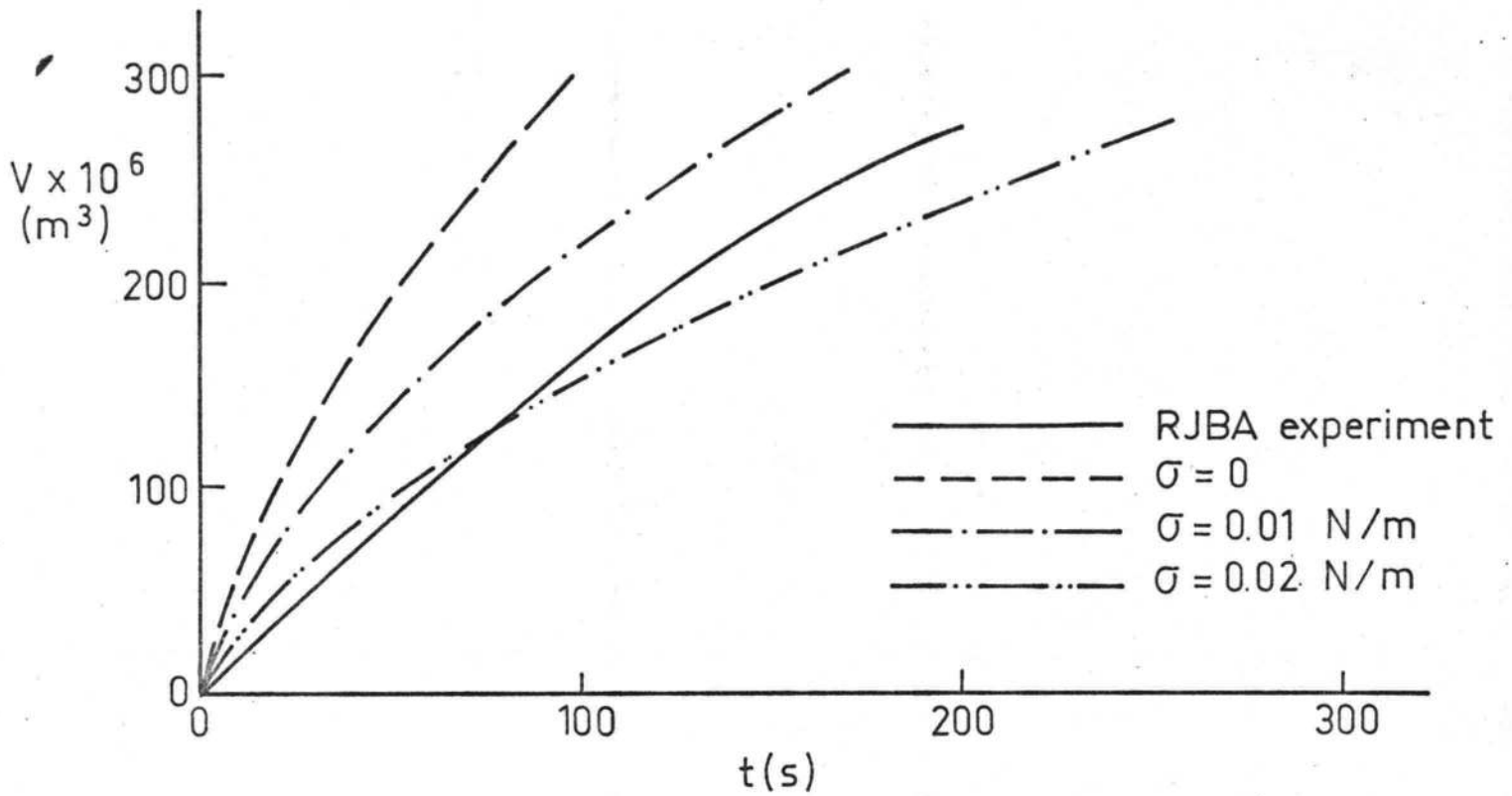

Fig. 4.6. Influence of interface tension on RJBA experiment.

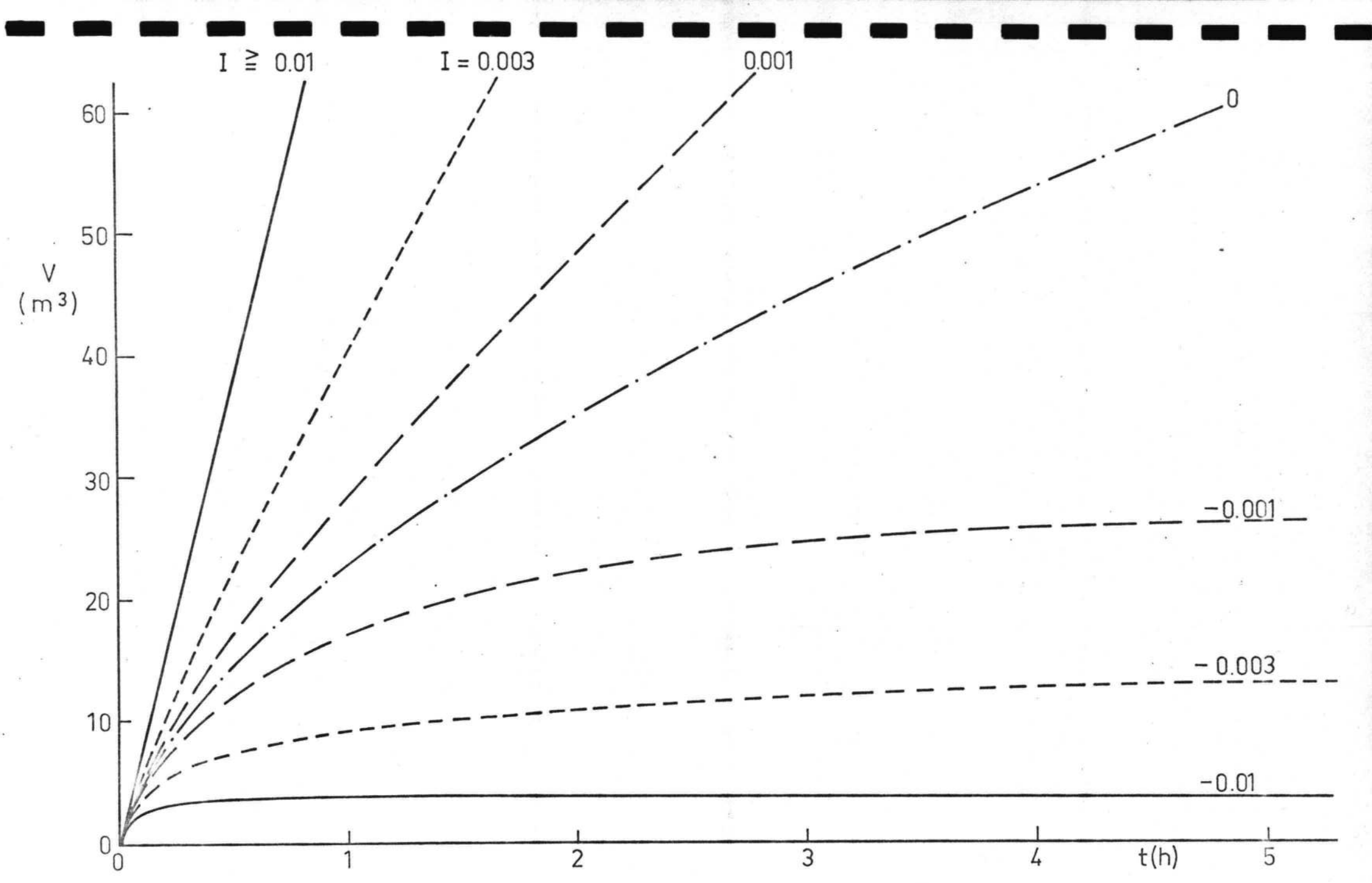

Fig. 5.1. Theoretical volume of leaked oil (prototype pipeline).